RadioGraphics Index terms:
Musculoskeletal Imaging
SPINE

Cumulative Index terms:
Spine, abnormalities

The vertebral body: Radiographic configurations in various congenital and acquired disorders

Rajendra Kumar, M.D.*

Faustino C. Guinto, Jr., M.D.*

John E. Madewell, M.D.†

Leonard E. Swischuk, M.D.*

Ruppert David, M.D.†

Many abnormal vertebral configurations are disease-specific and when recognized on radiographs, make correct diagnosis possible.

THIS EXHIBIT WAS DISPLAYED AT THE 73RD SCIENTIFIC ASSEMBLY AND ANNUAL MEETING OF THE RADIOLOGICAL SOCIETY OF NORTH AMERICA, NOVEMBER 29–DECEMBER 4, 1987, CHICAGO, ILLINOIS. IT WAS RECOMMENDED BY THE MUSCULOSKELETAL AND PEDIATRIC IMAGING PANELS AND WAS ACCEPTED FOR PUBLICATION AFTER PEER REVIEW ON MARCH 7, 1988.

From the Departments of Radiology, University of Texas Medical Branch, Galveston (*), and Baylor College of Medicine (†), Houston, Texas.

Address reprint requests to R. Kumar, M.D., Department of Radiology, University of Texas Medical Branch, Galveston, TX 77550.

Introduction

A normal vertebra has a body (centrum) and posterior elements. The body has a distinct shape and appears rectangular on radiographs. Its height tends to be somewhat less than its width. Many intrinsic and extrinsic disease processes may alter this normal vertebral body configuration. Such disorders may be congenital or acquired, often imparting specific shapes to the body (Table I). A knowledge of such abnormal vertebral body configurations may aid in the diagnosis of an underlying disorder.

The body of a vertebra is composed of cancellous tissue covered by a thin layer of compact bone, and contains numerous blood vessels. The trabeculae of the vertebra are more pronounced in the vertical than in the horizontal direction in response to greater stress along the cephalocaudal axis. Slight concavity normally characterizes all the surfaces of the vertebral body.

Table I
Classification of the Abnormal Configurations of the Body of a Vertebra

Congenital	Acquired
A. Asomia (agenesis)	A. Abnormal size
B. Hemivertebra	1. Small vertebral body
C. Coronal cleft	2. Enlarged vertebral body
D. Butterfly vertebra	B. Border abnormalities
E. Block vertebra	1. Anterior border scalloping
F. Hypoplasia	2. Posterior border scalloping
	3. Lateral border scalloping
	4. Anterior border straightening
	5. Endplate deformities
	C. Vertebral tongues, spurs and beaks
	D. Miscellaneous body shapes

Embryologic Considerations

The body of a vertebra develops from the cells of the sclerotome, a derivative of the notochord. Two ossification centers, one for the ventral and the other for the dorsal half of the body, appear by the 9th gestational week. Ossification of these centers is complete by the 12th week. These centers soon fuse to form a single large center which later divides the body of the future vertebra into two thick plates where endochondral ossification occurs. The portions of the notochord incorporated within the body undergo atrophy and disappear. Those which lie within the intervertebral discs enlarge and persist as the nuclei pulposi.

Any deviation in the normal development of the body of a vertebra leads to many congenital anomalies in its configuration, as illustrated in Figure 1.

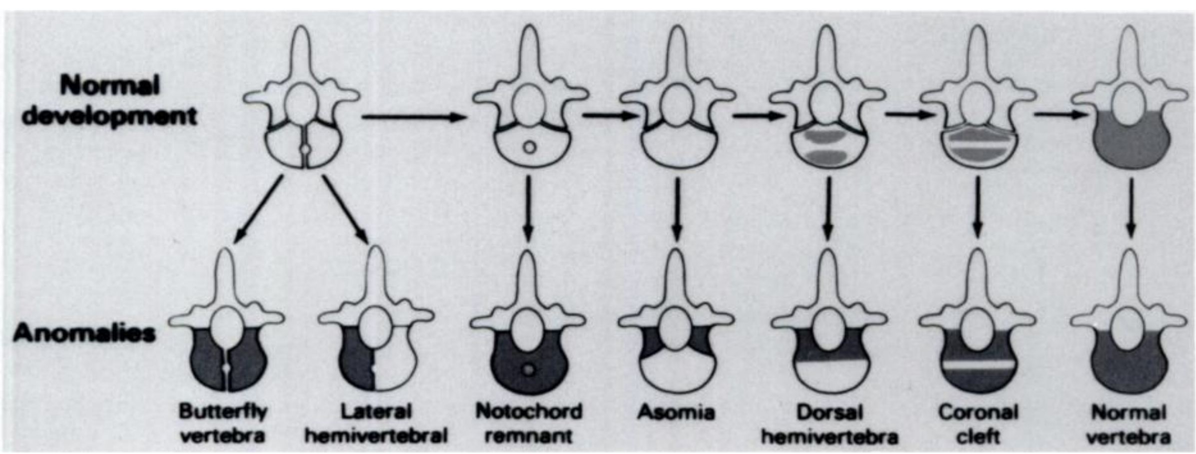

Figure 1
Schematic drawing depicting the development of normal and abnormal vertebral bodies.

Vertebral Body Configurations
Congenital

Developmental deformity of the body of a vertebra is often associated with congenital anomalies of the genitourinary, gastrointestinal, and central nervous systems.

A. Asomia (Agenesis)

Complete absence of the body of a vertebra may occur despite the presence of the posterior elements (Figure 2). This anomaly results from failure of ossification centers of the body to appear. One or more vertebral segments may be involved.

B. Hemivertebra

Unilateral wedge vertebra is due to lack of ossification of one-half of the body. A right or left hemivertebra may thus occur. The hemivertebra assumes a wedge-shaped configuration with the apex of the wedge reaching the midplane (Figure 3). Scoliosis is often present at birth.

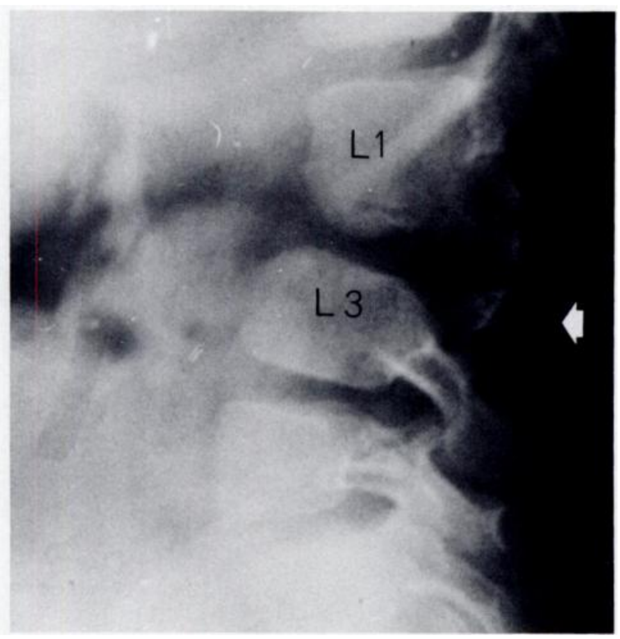

Figure 2
Asomia Congenital absence of the body of L2 Hypoplastic posterior elements are present (arrow).

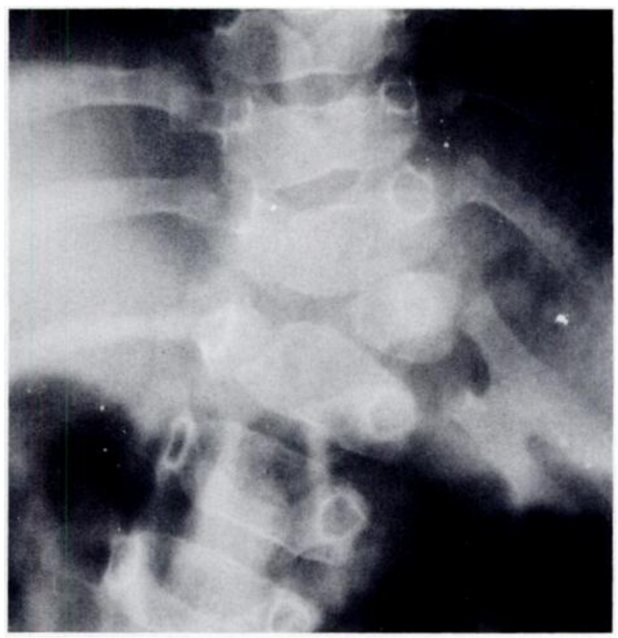

Figure 3
Left hemivertebra involving T11

Dorsal and ventral hemivertebrae occur because of failure of the ventral or dorsal half of the vertebral body to ossify (Figure 4). The failure of ossification is believed to be secondary to ischemia during the developmental stage. A kyphotic deformity is seen at the site of a dorsal hemivertebra. A ventral hemivertebra is extremely rare and results from failure of ossification of the dorsal half of the vertebral body.

Hemivertebra secondary to hemimetametric segmental displacement or persistence of the right and left halves of the vertebral body leads to the hemivertebrae being separated from each other in the sagittal plane. One such hemivertebra may fuse with the body of a vertebral segment above or below the affected segment (Figure 5).

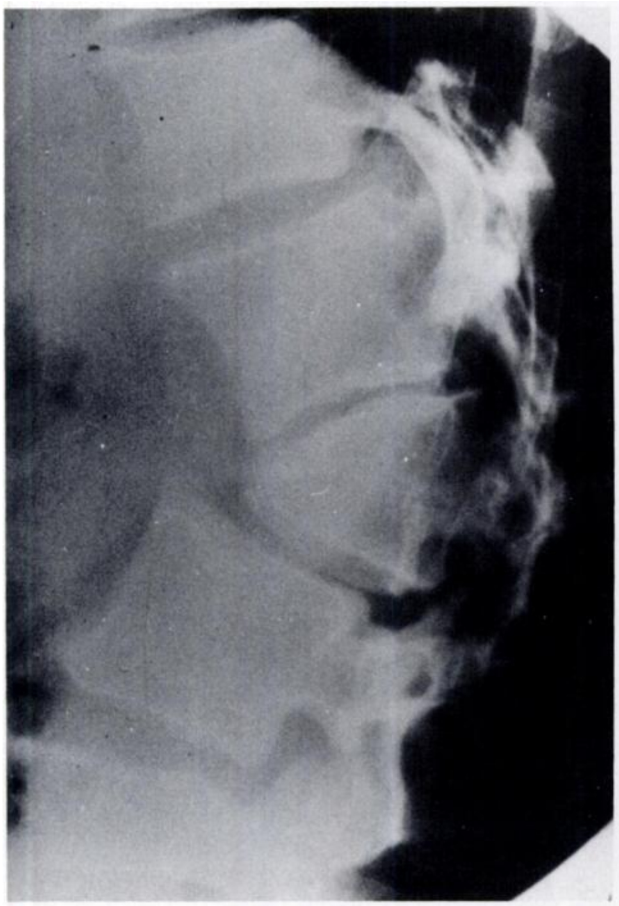

Figure 4
Dorsal hemivertebra involving L1

Figure 5
Metametric hemivertebrae in the lower lumbar spine with "mermaid" deformity of the lower extremities.

C. Coronal Cleft

This anomaly results from a failure of fusion of the anterior and posterior ossification centers which remain separated by a cartilage plate. It represents a delay in normal vertebral maturation; in most cases clefts disappear by six months after birth. Coronal clefts are usually seen in the lower thoracic or lumbar vertebral bodies. The deformity is most often seen in premature male infants and can be recognized *in utero*. Cleft vertebrae may also occur in infants with chondrodystrophia calcificans congenita. Radiographically, a vertical radiolucent band is seen just behind the midportion of the body on the laterial view of the spine (Figure 6).

D. Butterfly Vertebra
(Sagittal Cleft Vertebra)

Butterfly vertebrae result from the failure of fusion of the lateral halves of the vertebral body because of persistent notochordal tissue between them. The involved vertebral body is widened, and the bodies above and below the butterfly vertebra adapt to the altered intervertebral discs on either side by showing concavities along the adjacent endplates (Figure 7). Some bone bridging may occur across the defect which is usually seen in the thoracic or lumbar segments of the spine. Anterior spina bifida, with or without anterior meninogocele, may be associated with a butterfly vertebra.

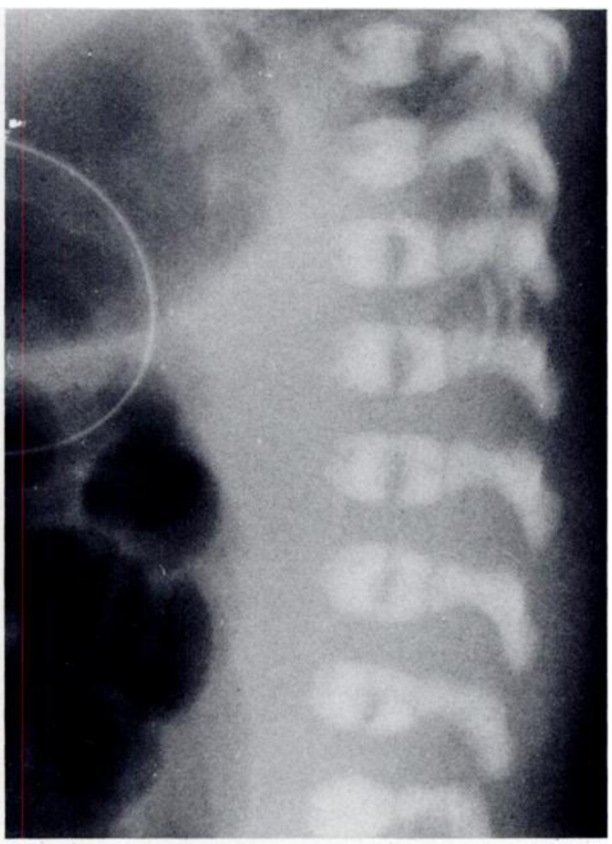

Figure 6
Vertebrae with coronal clefts are seen on this lateral view of the thoracolumbar spine.

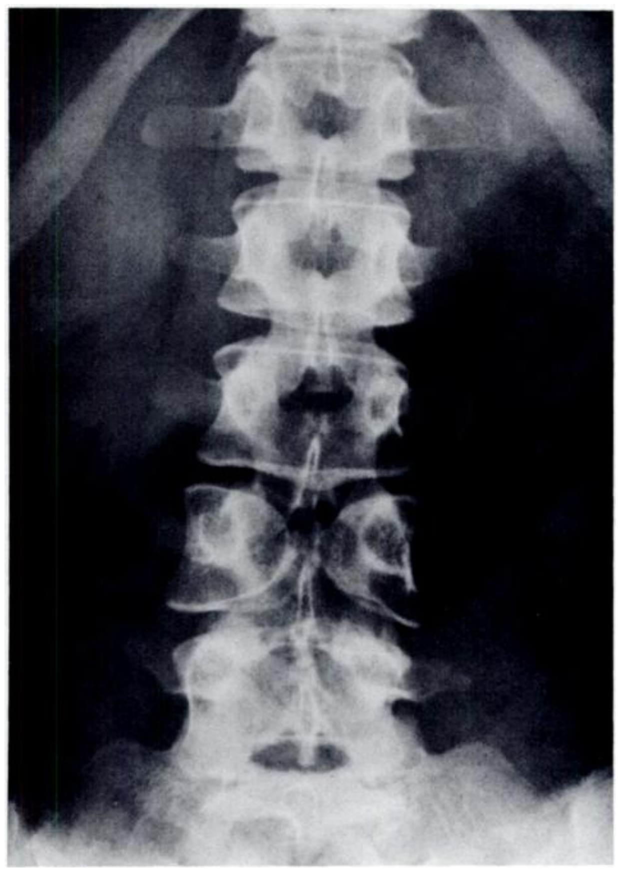

Figure 7
"Butterfly" vertebra involving L4

E. Block Vertebra
(Congenital Vertebral Fusion)

This congenital abnormality is due to a failure in the process of segmentation during fetal life. The fusion may be complete (both anterior and posterior elements involved), or partial. The height of fused bodies equals the sum of the heights of the involved bodies and the intervertebral discs between them. In acquired vertebral fusion, this dimension is less than in the case of congenital fusion. A "waist" is often seen at the level of the intervertebral disc between the fused segments (Figure 8A). This finding is usually absent in an acquired vertebral fusion (Figure 8B). The intervertebral foramina of block vertebrae become ovoid and narrowed. Congenital vertebral fusion usually occurs in the lumbar and cervical segments.

8A

8B

Figure 8
(A) **Block vertebra** with congenital fusion of C4 and C5 Note the presence of a "waist" at the site of fusion (arrow). (B) Acquired vertebral body fusion of C5 and C6.

F. Hypoplastic Vertebra

This anomaly is usually the result of vascular insufficiency during fetal life. It may affect one or more vertebrae (Figure 9).

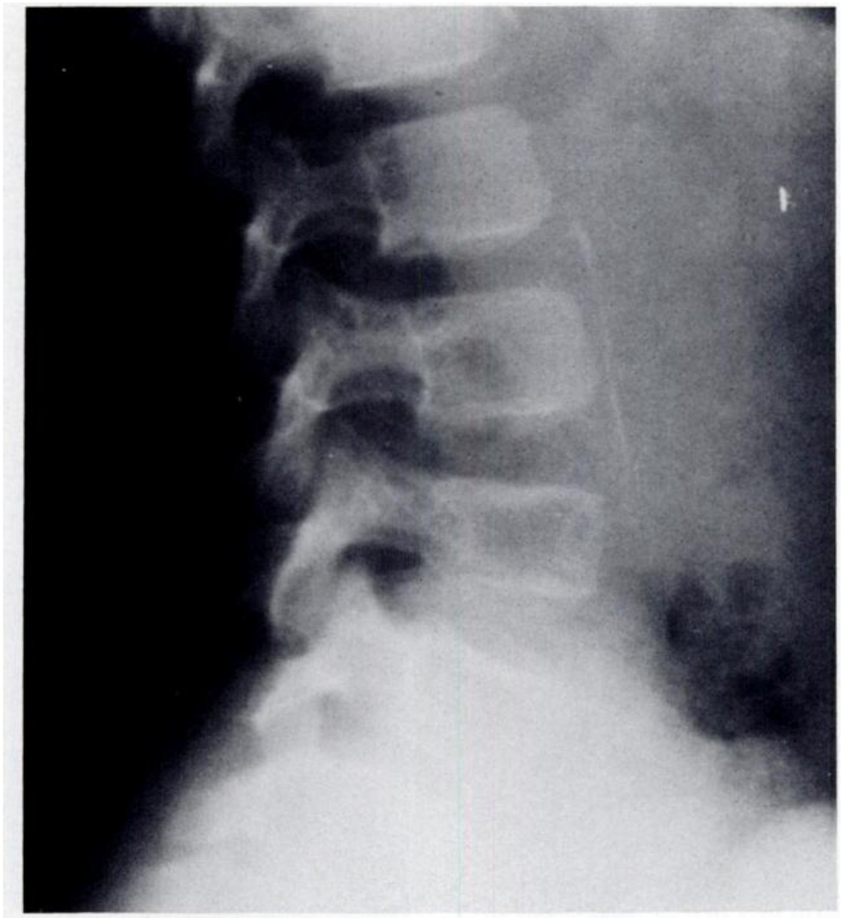

Figure 9
Congenital hypoplastic L4 vertebral body

Vertebral Body Configurations
Acquired

Vertebral body abnormalities resulting from trauma, infection, and neoplasm are excluded from this discussion.

A. ABNORMAL SIZE

An abnormality in the size of a vertebra is most often due to a compression deformity of the body. Certain diseases, however, may affect the normal vertebral growth resulting in altered size.

1. *Small Vertebral Body*

Radiation-induced vertebral hypoplasia may result from irradiation of the spine during early childhood (Figure 10). The effect is dose-dependent and, in general, does not occur with doses of less than 1000 rads. Unilateral radiation may cause scoliosis because of unequal growth of the affected bodies, the concavity of the scoliosis occurring on the irradiated side. Osteoporosis and vertebral collapse may be seen in adults following irradiation.

Juvenile rheumatoid arthritis causes reduced vertebral growth because of early epiphyseal closure; this results in small vertebrae (Figure 11). Vertebral fusion may also occur. The cervical spine is most often involved, and atlantoaxial subluxation may be present.

Figure 10
The left sided hypoplasia of the vertebral bodies seen here is due to unilateral irradiation of the lumbar spine for retroperitoneal hemangioma during childhood. Note the hypoplastic left kidney.

Figure 11
Juvenile rheumatoid arthritis with hypoplastic cervical vertebral bodies Note the posterior vertebral fusion.

Eosinophilic granuloma causes a marked compression deformity, and may lead to a "vertebra plana" deformity (Figure 12). Lesser compression deformities are more frequent, however. The lumbar and lower thoracic portions of the spine are most often involved. This is a self-limiting disease. The vertebra may regain "normal" shape after many years, with or without treatment.

Gaucher's disease is characterized by the deposit of glucocerebrosides within the reticuloendothelial cells of the vertebral body. This causes weakening and compression deformity similar to that seen in osteoporosis (Figure 13).

Figure 12
Eosinophilic granuloma with typical "vertebra plana" involving T12

Figure 13
Gaucher's disease with osteoporosis and compression deformities of vertebral bodies

Platyspondyly generalizata is a nonspecific descriptive term applied to the many hereditary systemic diseases that are associated with flattened vertebral bodies. Though vertebral bodies are flat, the discs tend to be of normal height. Dwarfism and numerous spinal curvature deformities may be present. Such flat vertebral bodies have been described in achondroplasia, spondyloepiphyseal dysplasia tarda (Figure 14), mucopolysaccharidosis, osteopetrosis, neurofibromatosis, osteogenesis imperfecta (Figure 15), and many others.

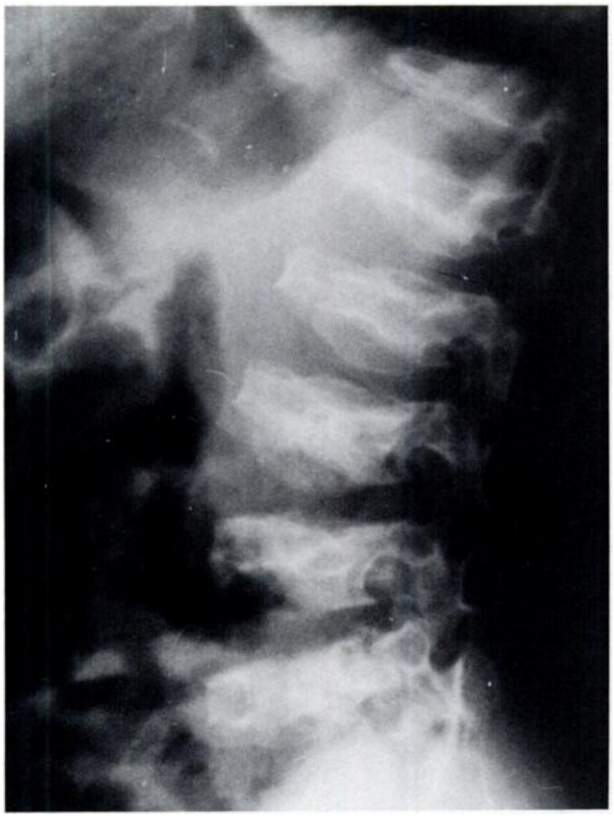

Figure 14
Platyspondyly in spondyloepiphyseal dysplasia tarda

Figure 15
Osteogenesis imperfecta tarda with osteoporosis and compression deformities of vertebral bodies

Thanatophoric dwarfism results in extreme flattening of the hypoplastic vertebral bodies (Figure 16A). An "H" or "U" configuration of the vertebral bodies is seen in the anteroposterior view (Figure 16B).

16A

16B

Figure 16
(A) Thanatophoric dwarf with marked platyspondyly of hypoplastic vertebral bodies (B) "H" and "U" configurations of the vertebral bodies are seen in this AP view.

2. Enlarged Vertebral Body

Paget's disease causes enlargement of the vertebral body in all dimensions unless complicated by a compression fracture. A "picture-frame" appearance may be imparted to the body in the mixed phase of the disease (Figure 17). The body alone or the entire vertebra may be involved and often appears sclerotic.

Gigantism may cause an increase in the height of vertebral bodies (Figure 18). The intervertebral discs may show a similar change.

Myositis ossificans progressiva produces vertebral bodies that are tall, being greater in height than in width (Figure 19). Associated osteoporosis may ultimately lead to compression deformity of the vertebral bodies.

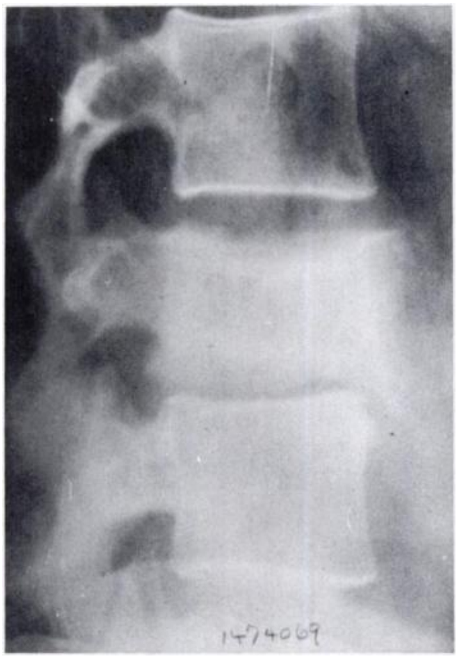

Figure 17
Paget's disease showing enlargement of the L3 vertebral body with the "picture-frame" vertebra appearance

Figure 19
Myositis ossificans progressiva with "tall but slim" vertebrae in the cervical spine Note the ossification of the ligamentum nuchae (arrowhead).

Figure 18
Gigantism with "tall" vertebral bodies in the cervical spine

B. BORDER ABNORMALITIES

Any border of a vertebral body, including the end plates, may be affected.

1. Anterior Border Scalloping

Aortic aneurysm because of its pulsatile pressure may cause a concave compression defect along the anterior surface of an adjacent vertebral body (Figures 20A and B). The defect has a sclerotic margin, consistent with the chronicity of the process. The lower thoracic and upper lumbar vertebral segments are most often involved.

20A

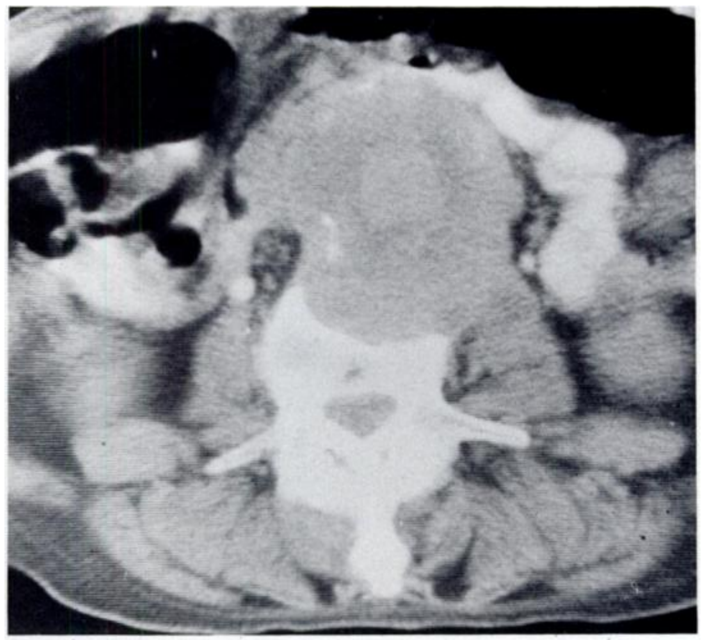

20B

Figure 20
(A) This lateral tomogram of the lumbar spine shows anterior vertebral notching (arrows) of L2 and L3. (B) A CT section through L3 shows that the anterior vertebral notching is caused by a large abdominal aortic aneurysm. Note the contrast enhanced lumen of the enlarged aorta in the center and the calcification in the wall of the aneurysm. (Courtesy of N. Patel, M.D., Newburgh, NY.)

2. Posterior Border Scalloping

Normal posterior scalloping may occur as a rare variant. In contrast to the concave defect seen with other disorders, the posterior scalloping that represents a normal variant is characterized by an angular defect with its apex pointing anteriorly (Figure 21).

Neurofibromatosis is associated with marked scalloping of the posterior borders of the vertebral bodies caused by dural ectasia or intraspinal tumors (Figures 22A and B). Widening of the intervertebral foramina may be seen. Any spinal segment may be involved, and scoliosis and kyphoscoliosis may be present. Rarely, anterior border scalloping may be seen in neurofibromatosis.

Figure 21
Normal posterior vertebral notching in the lumbar spine

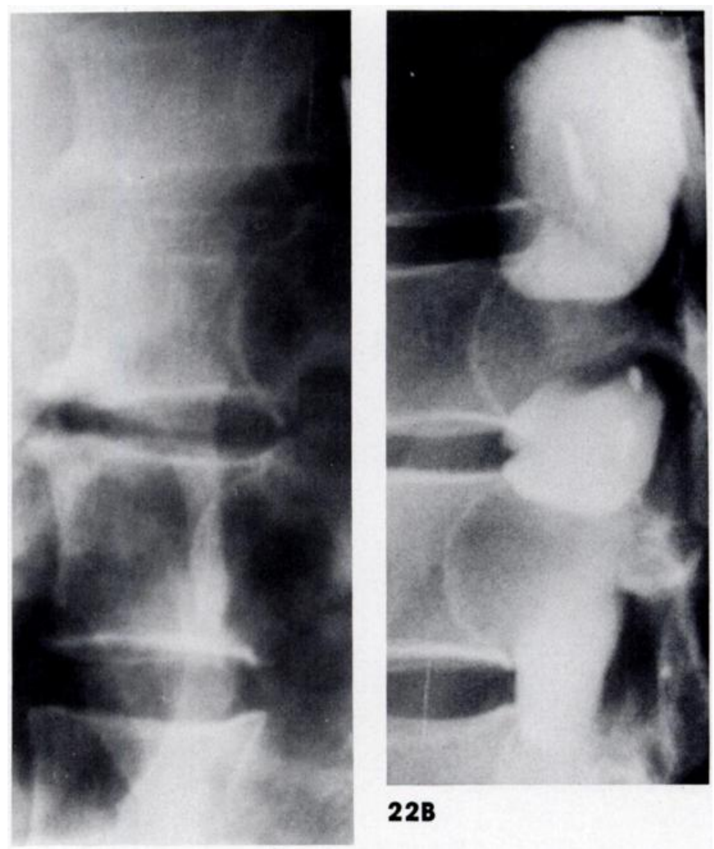

22B

22A

Figure 22
(A) **Neurofibromatosis** with posterior vertebral notching in the lumbar spine (B) A myelogram shows that the vertebral notching is secondary to dural ectasia.

In *achondroplasia,* posterior indentation of the vertebral bodies may be present owing to a developmental defect (Figure 23). Platyspondyly is often seen. Disc herniations with marked spondylosis deformans are frequently seen in older patients.

In *acromegaly,* scalloping is often present along the posterior aspect of lumbar vertebrae (Figure 24), and the anteroposterior diameter of the bodies may be increased in the thoracic spine. Diffuse osteoporosis is common with compression deformities of the vertebral bodies. Marked spondylosis deformans may be present.

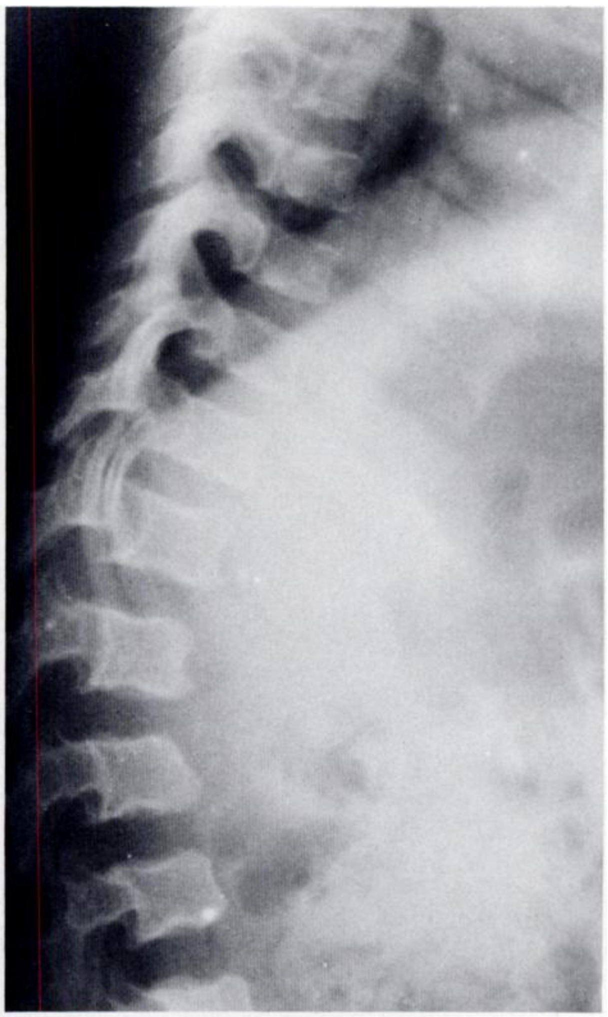

Figure 23
Achondroplasia with posterior vertebral notching in the thoracolumbar spine

Figure 24
Acromegaly with posterior vertebral notching in the lumbar spine

Ependymoma ("Dog Spine") usually originates in the filum terminale and produces scalloping along the posterior borders of lumbar vertebral bodies (Figure 25). Rarely, the lower thoracic vertebrae may be involved. There is also widening of the spinal canal with thinning and spreading of the vertebral pedicles (any large intraspinal tumor or dural ectasia can produce similar defects).

Posterior meningocele (Spina bifida cystica) most often occurs in the lumbar and sacral regions. Posterior concave vertebral indentations occur as a result of compression by the meningocele (Figure 26). Widening of the spinal canal with spreading and thinning of vertebral pedicles is also seen, and spina bifida and other congenital vertebral anomalies are often present. Both posterior and anterior meningoceles may occur in neurofibromatosis.

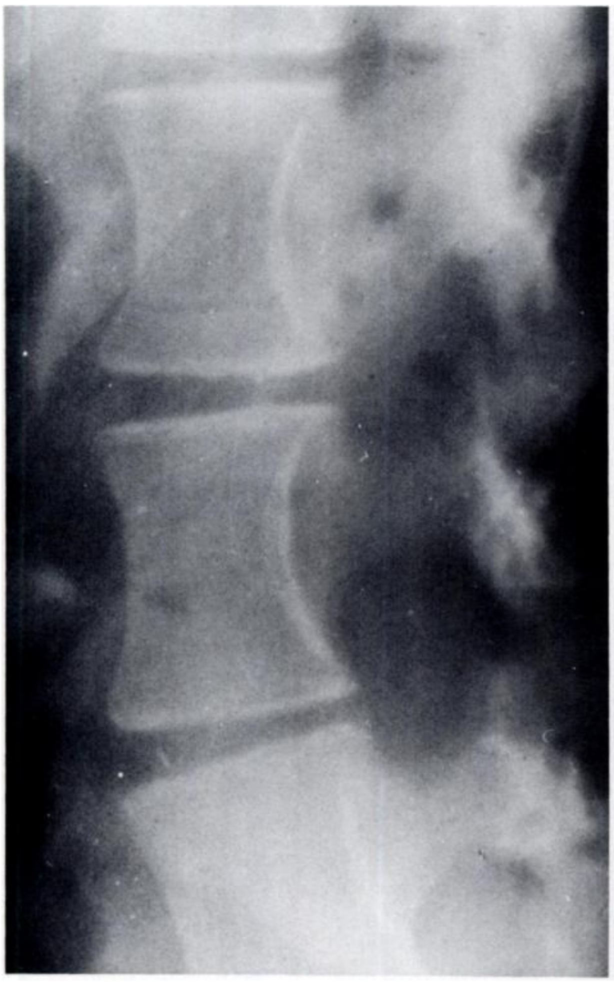

Figure 25
Ependymoma with posterior vertebral notching in lumbar vertebral bodies ("Dog spine")

Figure 26
Meningocele with posterior vertebral notching in the mid thoracic spine (arrows)

3. Lateral Border Scalloping

Any benign mass that lies in close proximity to either side of the vertebral column may cause indentations along the lateral borders of vertebral bodies. This may be seen in neurofibromatosis, for example (Figure 27).

4. Anterior Border Straightening

Ankylosing spondylitis produces a "square" or "box-like" vertebral body configuration in the early stages of the disease, owing to straightening of the anterior border (Figure 28). This, in turn, is the result of bone erosions at the anterior corners of the body resulting in loss of the normal concavity of the anterior vertebral surface. This finding is best seen in the lumbar spine.

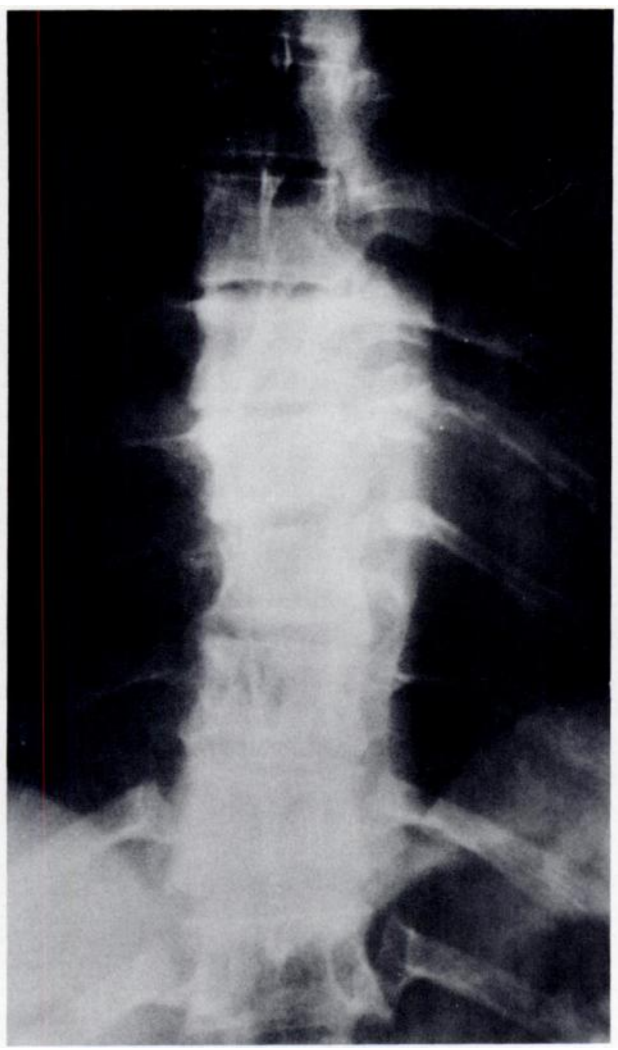

Figure 27
Neurofibromatosis Vertebral notching caused by neurofibromas is seen along the right lateral borders in the thoracic spine.

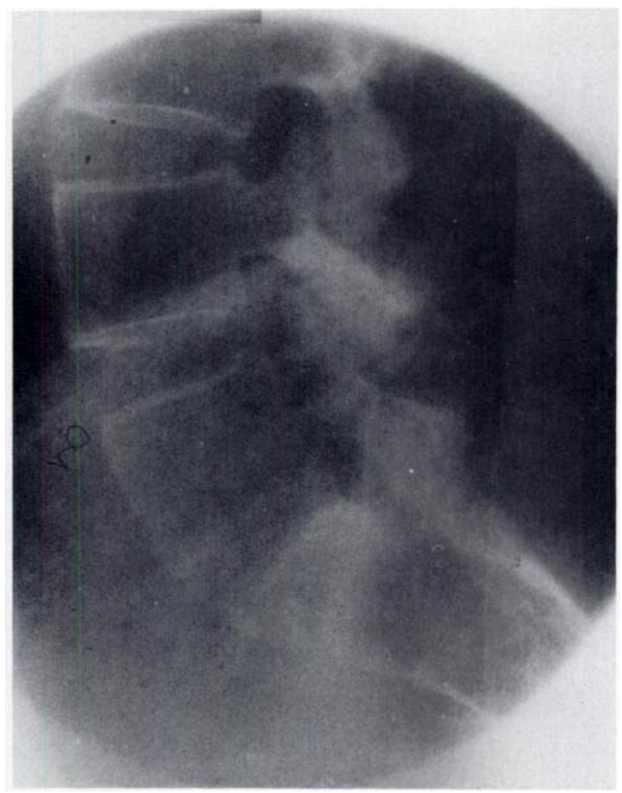

Figure 28
Ankylosing spondylitis with straightening of the anterior borders of the lumbar vertebral bodies

5. Endplate Abnormalities

Osteoporosis occurs in many disorders and results in weakening and collapse of the vertebral body. It is often seen in postmenopausal women. Compression deformity of one or more vertebral bodies may occur with decrease in the vertebral height, and ultimately wedge-shaped, flat or biconcave vertebral bodies ("fish vertebra") may result (Figures 29A and B).

29A

29B

Figure 29
Osteoporosis (A) "Fish-vertebrae" with biconcave deformities of lumbar vertebral bodies (B) Normal spine of a fish showing biconcave vertebrae

Steroid-induced osteoporosis occurring in patients who have Cushing's syndrome or who are on exogenous steroid therapy is a generalized process. In the spine, compressed vertebral bodies resulting from the osteoporosis may show bone condensation along the superior and inferior endplates (Figure 30), a feature infrequently seen with compressed osteoporotic vertebrae resulting from other causes.

Sickle cell disease causes a step-like central depression of the vertebral endplates that results in the appearance of an "H vertebra" (Figure 31). Compression of the central portions of the endplates occurs because of subchondral bone infarcts in the vertebral body. The body, because of infarction, is usually nonhomogeneous in appearance. The integrity of the peripheral endplates is believed to be preserved by a collateral blood supply. The disc spaces may be narrowed. Similar step deformities may also be seen in mixed hemoglobinopathies.

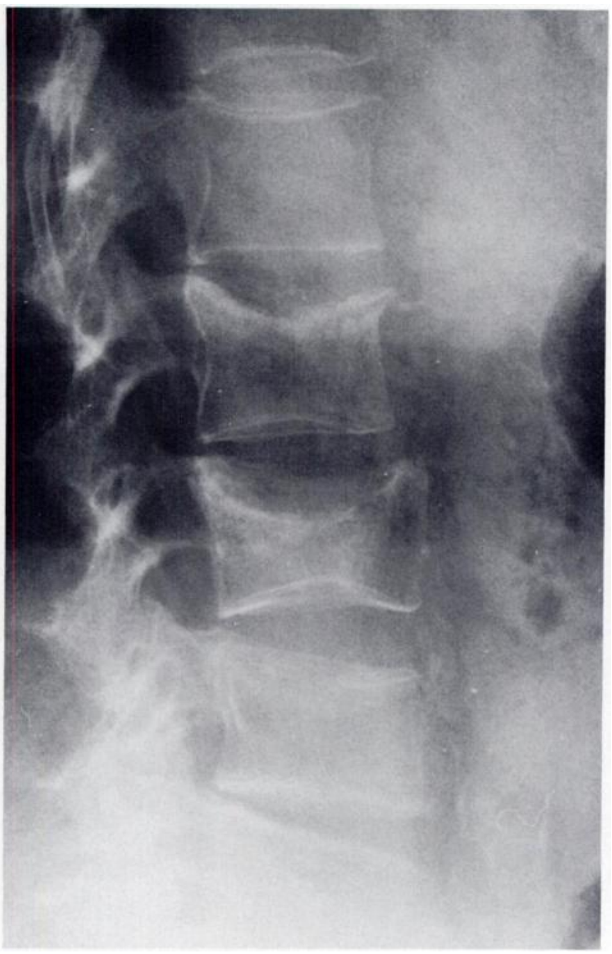

Figure 30
Steroid induced osteoporosis with vertebral compression deformities Note the increased sclerosis subjacent to the deformed superior endplates.

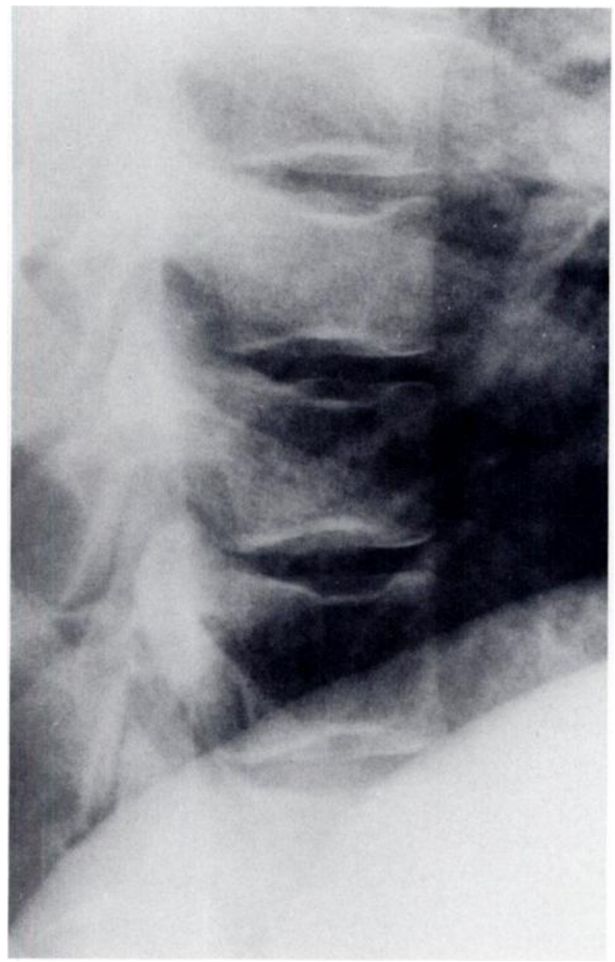

Figure 31
Sickle cell anemia with "step-off" deformity of vertebral endplates ("H" vertebra) in the thoracic spine

A *Schmorl's node* is a contour defect in the endplate of a vertebra resulting from central herniation of a portion of the disc into the adjacent vertebral body (Figures 32A and B). A defect or weakness in the endplate leads to such disc herniation. A Schmorl's node is seen as a radiolucent defect with a sclerotic margin subjacent to the vertebral endplate.

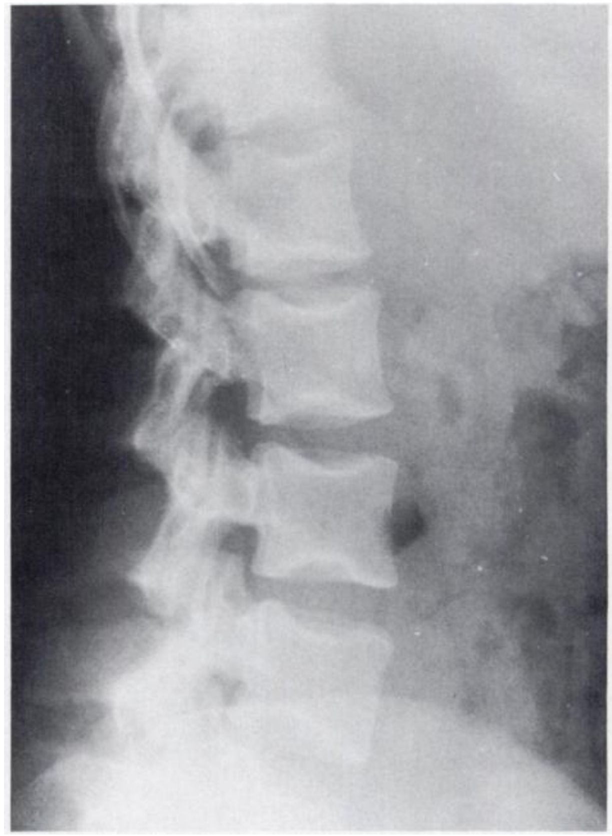

32A

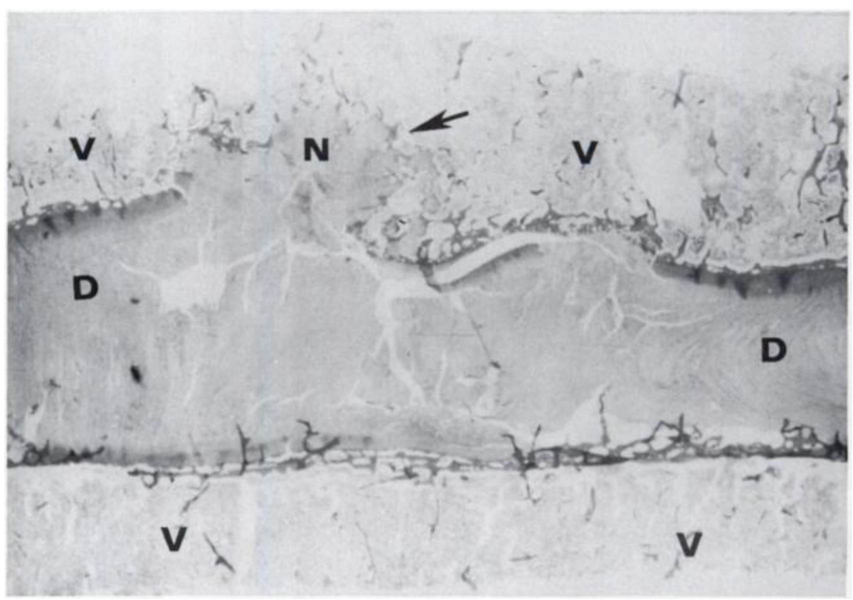

32B

Figure 32
(A) **Schmorl's nodes** deforming lumbar vertebral endplates (B) This photomicrograph shows central herniation of the nucleus pulposus into the adjoining vertebra, resulting in a Schmorl's node formation. D = disc; N = nucleus pulposus; V = vertebral body

A *limbus vertebra* represents a distinct type of disc herniation in which there is intraosseous penetration of disc material at the junction of the endplate with the vertical bony rim of a vertebral body. An oblique radiolucent defect is seen coursing toward the outer surface of the vertebral body which separates a small segment of the bone (Figure 33). It most often occurs at the anterosuperior corner of a single lumbar vertebra.

A *"ring" epiphysis* is a cartilaginous ring around the superior and inferior margins of a vertebral body. They represent a normal aspect of the development of a vertebra, and are seen as small, step-like recesses at the corners of the anterior edges of vertebral bodies in patients 6 to 9 years of age (Figure 34). Later, the entire ring may calcify. The fusion of the ring epiphyses to the vertebral body is complete by 12 years of age.

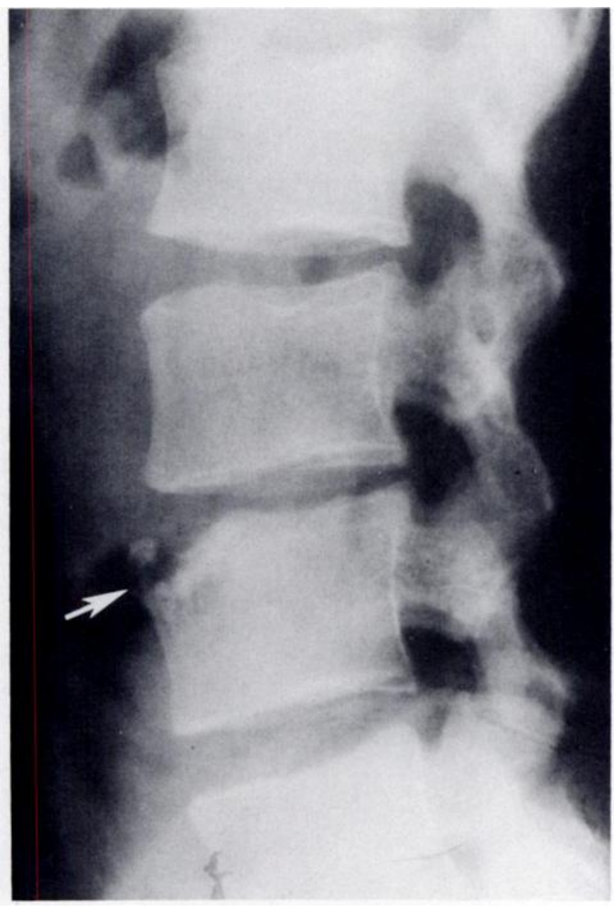

Figure 33
Limbus vertebra Note the radiolucent defect at the anterosuperior border of L4 (arrow).

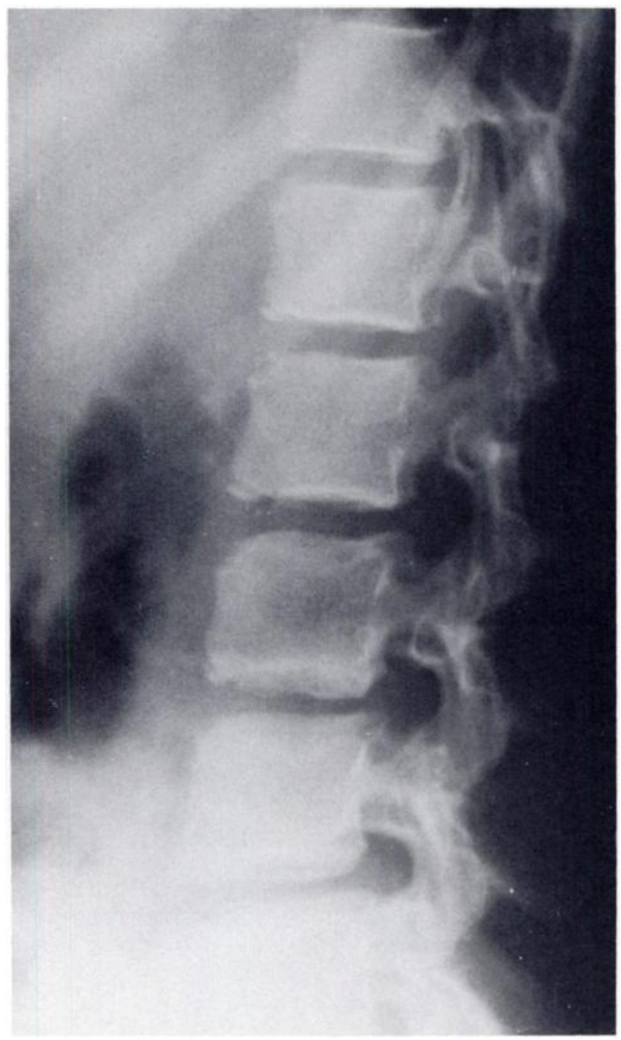

Figure 34
Normal "ring" epiphyses of the thoracic and lumbar vertebral bodies

Renal osteodystrophy is characterized by the presence of horizontal bands of increased opacity subjacent to the endplates of vertebrae. These zones of sclerosis alternate with radiolucent bands through the centers of the vertebral bodies and the radiolucent disc spaces, imparting a "rugger-jersey" appearance to the spine. The sclerotic bands are believed to be due to condensation of excessive osteoid adjacent to the endplates. The "rugger-jersey" appearance is usually seen in renal osteodystrophy (Figure 35), but may occur in osteopetrosis (Figure 36) and myelofibrosis.

Figure 35
Renal osteodystrophy with the "rugger-jersey" appearance of the lumbar spine

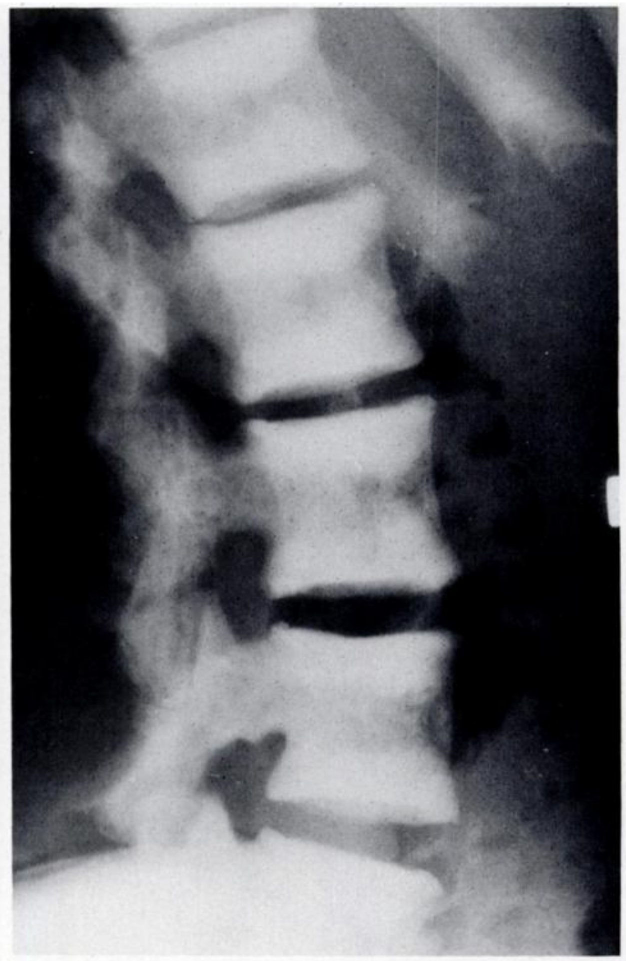

Figure 36
Osteopetrosis in an adult showing a "rugger-jersey" lumbar spine

In *osteopetrosis,* sclerotic vertebral end-plates alternate with the radiolucent regions of the disc spaces and the midportions of the vertebral bodies, producing a "sandwich" vertebra or "hamburger" vertebra appearance in children (Figure 37). A "rugger-jersey" spine may be seen in adults (Figure 36).

Figure 37
Osteopetrosis in a child showing "sandwich" vertebrae

C. VERTEBRAL TONGUES, BEAKS AND SPURS

Various bony projections may arise along the vertebral margins. Some of these projections impart specific contours to vertebral bodies.

In *Hurler's syndrome (Gargoylism),* vertebral bodies have a rounded appearance. A mild kyphotic curve is seen at the thoracolumbar junction. The body at the apex of the kyphotic curve is somewhat smaller than the adjacent bodies and is deficient in its anterosuperior aspect. As a result, its lower half projects anteriorly in a tongue-like fashion (Figure 38). Usually, it is the body of T12, L1 or L2 that is involved. Similar but less severe changes are often seen in Hunter's syndrome.

Figure 38
Hurler's syndrome with "step-off" deformities along the anterior margins of the lumbar vertebral bodies

In *Morquio's disease,* the vertebral bodies are markedly flattened and widened and anterior "tongue-like" elongations of their central portions are seen (Figure 39). The endplates of the bodies are coarse and irregular. Disc spaces may appear normal or somewhat widened. Usually the entire vertebral column is involved, and a kyphoscoliosis may be present.

In *hypothyroidism,* the vertebral bodies tend to be small and flat. Anterior "tongue-like" deformities of the vertebral bodies are present in children (Figure 40A). The disc spaces are widened and the endplates may be irregular. With treatment, most vertebral changes tend to disappear, and only minor residual deformity of the vertebral bodies remains in the adult (Figure 40B).

Figure 39
Morquio's disease with central beaking along the anterior margins of the thoracolumbar vertebral bodies

40A

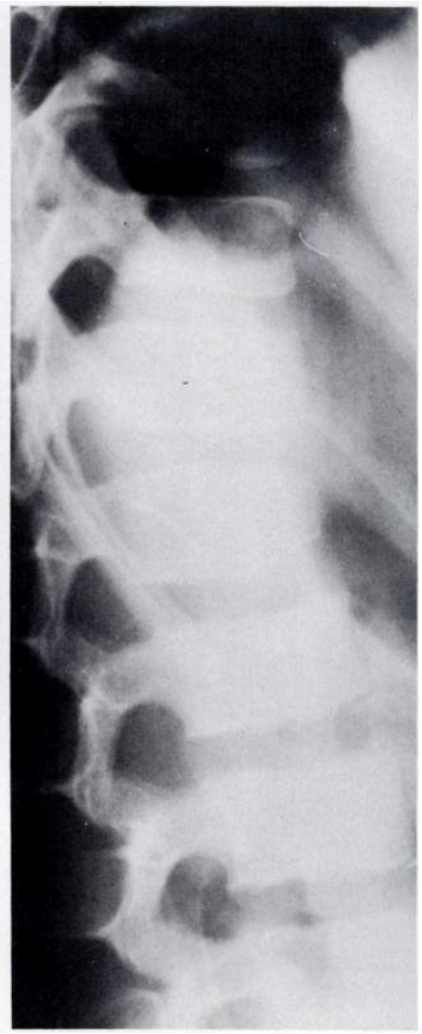

40B

Figure 40
(A) **Cretinism** with central beaks along the anterior vertebral borders (B) Following treatment, the same patient years later shows minimal residual vertebral deformities.

Spondylosis deformans represents degenerative disc disease and is most often seen in older persons. Osteophytes occur as a result of the shearing of the outer annular (Sharpey's) fibers, which connect the annulus fibrosus to the adjacent vertebral bodies. These fibers are ruptured with disc herniation which separates the overlying anterior and longitudinal spinal ligaments from the vertebral bodies. Reactive bone formation at these sites of disruption results in the formation of horizontal and vertical osteophytes. The osteophytes arise along the anterior and lateral aspects of the vertebral bodies (Figures 41A and B). Osteophytes along the posterior aspect of the vertebral body are rare.

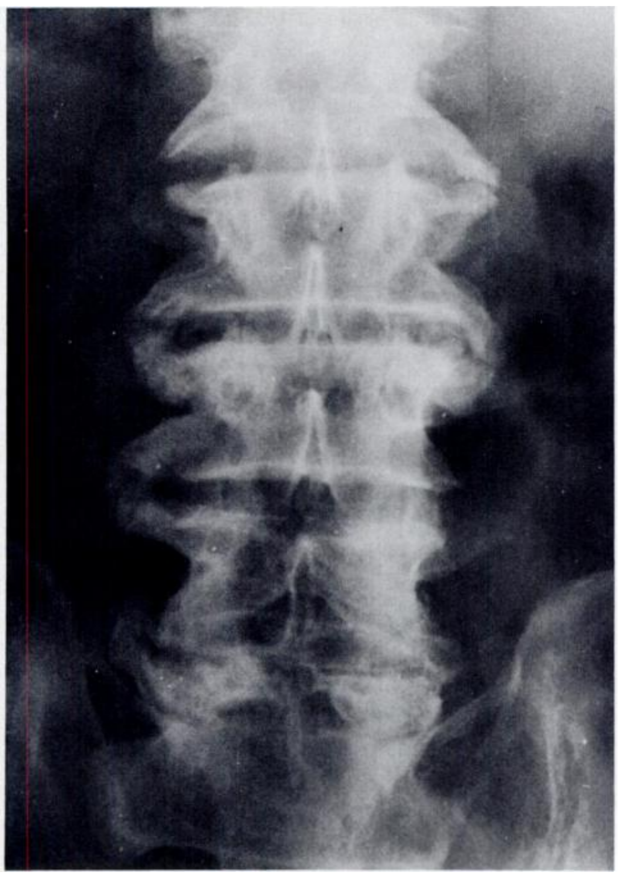

41A

41B

Figure 41
Spondylosis deformans with osteophytosis in the anteroposterior (A) and lateral (B) views

Diffuse idiopathic skeletal hyperostosis (DISH) *(Forestier's disease)* is defined as flowing calcification and ossification along the anterolateral aspects of at least four contiguous thoracic vertebral bodies with or without osteophytosis (Figure 42). Relative preservation of the disc spaces of the affected vertebrae is often seen. It most often affects the thoracic spine but may involve any spinal segment.

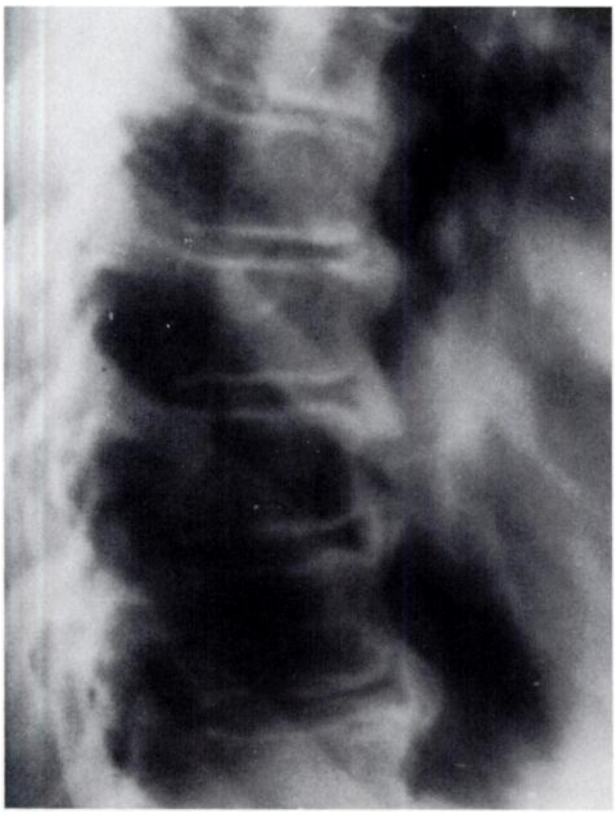

Figure 42
Diffuse idiopathic skeletal hyperostosis involving the thoracic spine with ossification of the anterior longitudinal ligament

In *ankylosing spondylitis,* bilaterally symmetrical syndesmophytes occur because of ossification of the annulus fibrosus. A "bamboo spine" appearance is typically seen as a result of extensive syndesmophytosis (Figure 43). "Discal ballooning" producing biconvex intervertebral discs may be present owing to osteoporotic deformity of the endplates. Straightening of the anterior margins of vertebral bodies occurs because of bone erosions at the anterior corners of the bodies (Figure 28). Ossification of paraspinal ligaments is also seen.

Figure 43
Ankylosing spondylitis with a "bamboo" spine resulting from symmetrical syndesmophytosis on an anteroposterior view of the lumbar spine

In *fluorosis*, vertebral osteophytosis and hyperostosis with sclerotic vertebral bodies are often seen. Calcification of paraspinal ligaments may occur, kyphoscoliosis of the spine may be present, and neurological deficits may occur in advanced cases.

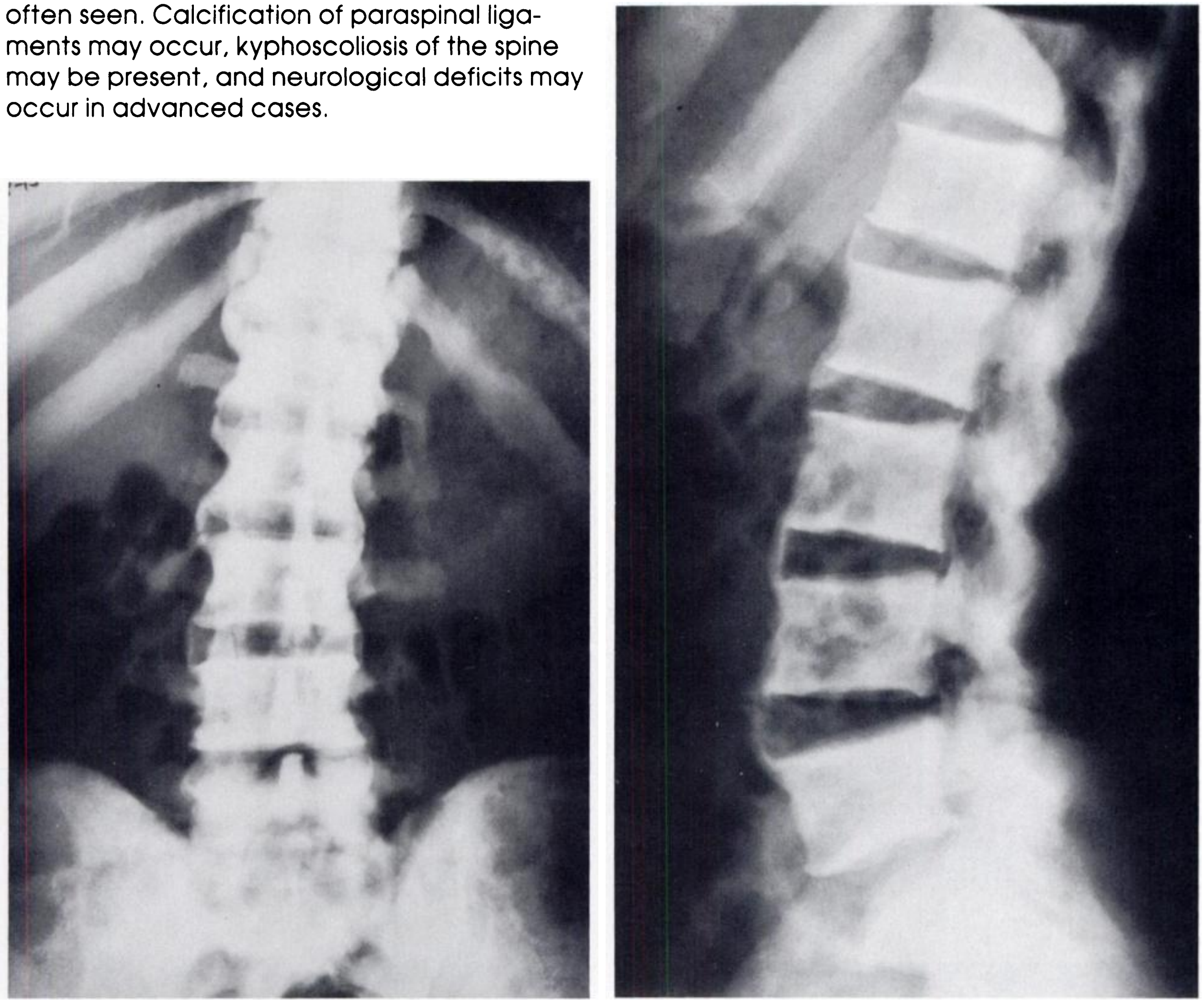

44A **44B**

Figure 44
Fluorosis Anteroposterior (A) and lateral (B) views of a lumbar spine show ossification of the paraspinal longitudinal ligaments.

D. MISCELLANEOUS CONFIGURATIONS

Hemangioma is most often seen in the lower thoracic and upper lumbar portions of the spine. Thickening of the vertical bony trabeculae in the body produces what has been called the "accordion" or "corduroy" appearance of the involved vertebral body (Figures 45A and B). A similar appearance may, at times, be seen with osteoporosis (Figure 46). One or more vertebrae may be involved.

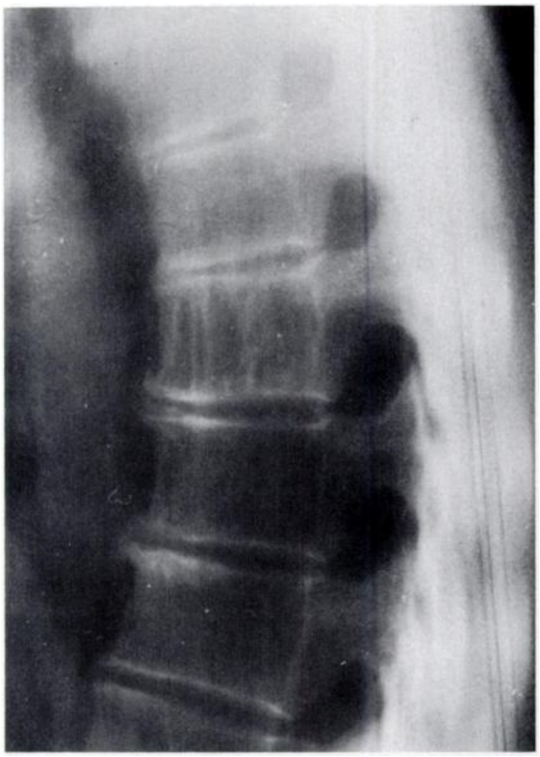

45A

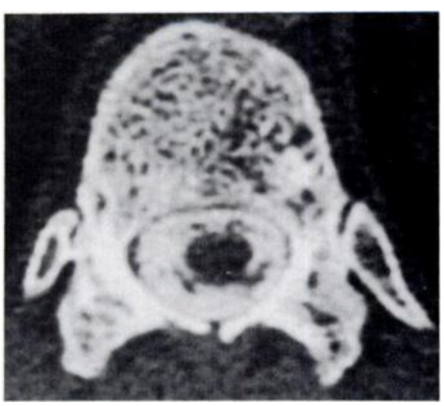

45B
Figure 45
(A) **Hemangioma** involving the T8 vertebral body
(B) CT shows that the "honey-comb" appearance of the body is caused by coarse bone trabeculae.

Figure 46
Osteoporosis mimicking vertebral hemangiomas
Note the fine vertical striations in the lumbar vertebral bodies.

"Bone-within-bone" vertebra (ghost vertebra) occurs following a stressful event during vertebral growth in childhood (Figures 47A and B). Thin transverse lines parallel to the vertebral endplates represent "poststress", "recovery", or "regrowth" phenomena. Once formed, the lines persist throughout life (Figure 48). Various causes of the "bone-within-bone" vertebra are listed in Table II.

Figure 47
"Bone-within-bone" vertebra Anteroposterior (A) and lateral (B) views of the lumbar spine show "stress lines" of unknown cause along the endplates of the vertebral bodies.

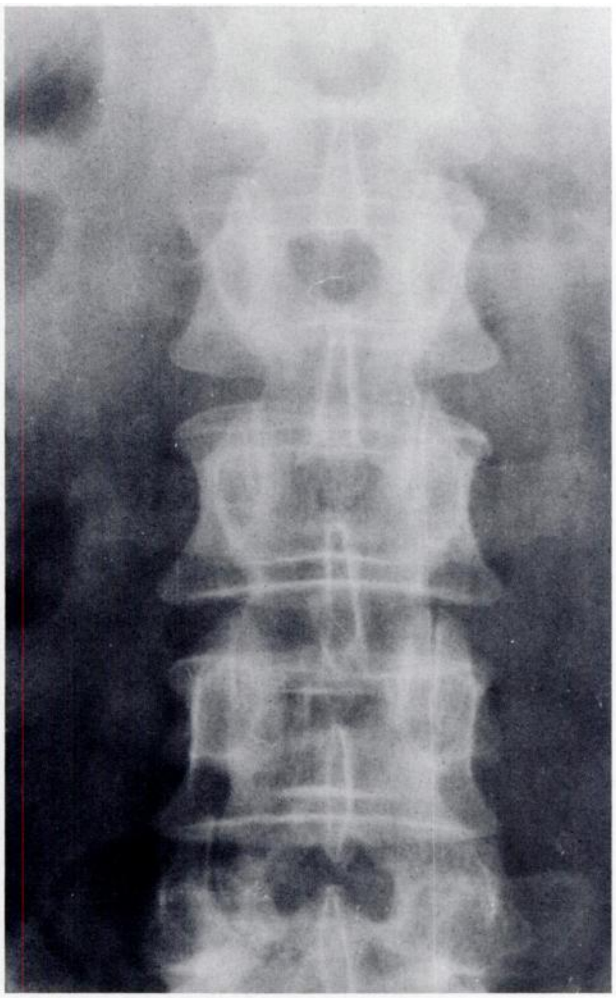

47A

47B

Table II
Causes of Ghost Vertebra

Stress line	Rickets
Leukemia	Scurvy
Heavy metal poisoning	Hypothyroidism
Thorotrast injection	Hypoparathyroidism

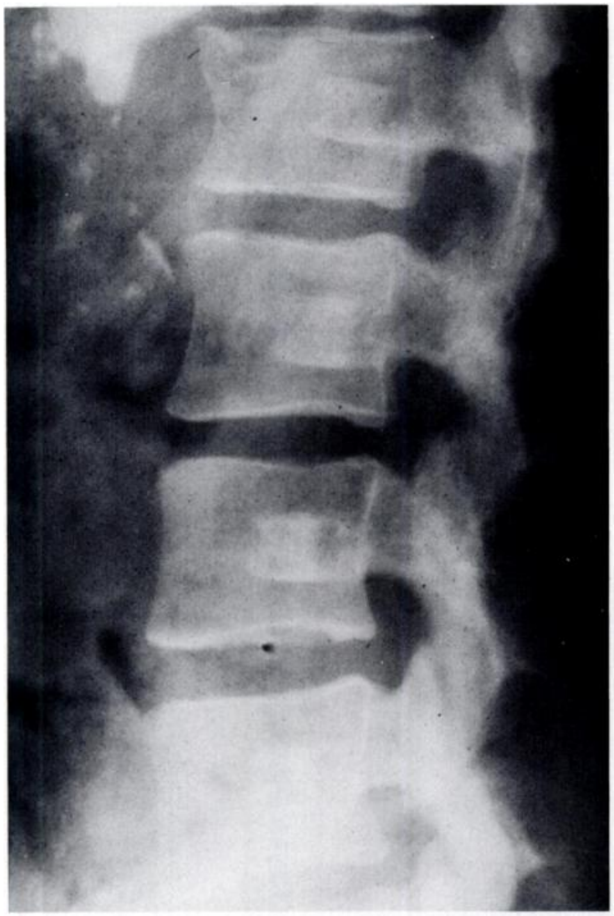

Figure 48
"Bone-within-bone" appearance of lumbar vertebral bodies resulting from Thorotrast administration The inner, infantile vertebral body represents vertebral body size at 2 years of age when Thorotrast was administered.

The *"Napolean hat"* sign, seen on an anteroposterior radiograph, represents a grade IV spondylolisthesis of L5 over S1 (Figures 49A and B).

49A

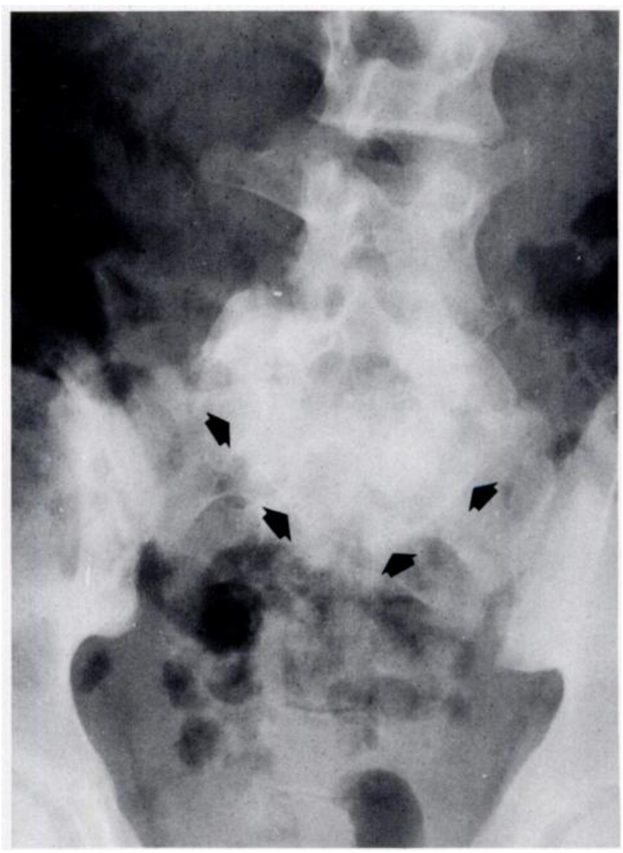

49B

Figure 49
(A) **Spondylolisthesis** (Grade IV) of L5 on S1 on a lateral view (B) The inverted "Napoleonic hat" sign (arrows) on an anteroposterior view of the pelvis

Conclusion

The body of a vertebra may assume many different configurations. Some of these contour changes are disease-specific. Recognition of these vertebral body configurations greatly facilitates radiographic diagnosis.

Suggested Readings

1. Barone BM, Elvidge AR. Ependymomas: A clinical survey. J Neurosurg 1970; 33:428–438.
2. Berens DL. Roentgen features of ankylosing spondylitis. Clin Orthop 1971; 74:20–33.
3. Caffey J. Achondroplasia of the pelvis and lumbosacral spine. Some roentgenographic features. AJR 1958; 80:449–457.
4. Compere EL, Johnson WE, Caventry MG. Vertebra plana (Calve' disease) due to eosinophilic granuloma. J Bone Joint Surg [Am] 1954; 36:969–980.
5. Epstein BS. The spine. A radiological text and atlas. 4th ed. Philadelphia: Lea & Febiger, 1976.
6. Gjorup PA. Dorsal hemivertebra. Acta Orthop Scand 1964; 35:117–125.
7. Lang EK, Bessler WT. The roentgenographic features of acromegaly. AJR 1961; 86:321–328.
8. Langer LO, Jr. Spondyloepiphyseal dysplasia tarda: Hereditary chondrodysplasia with characteristic vertebral configuration in the adult. Radiology 1964; 82:833–839.
9. Langer LO Jr, Carey LS. The roentgenographic features of the KS mucopolysaccharidosis of Morquio (Morquio-Brailsford Disease). AJR 1966; 97:1–20.
10. Levin EJ. Osteogenesis imperfecta in the adult. AJR 1964; 91:973–978.
11. Lonstein JE. Embryology of the spinal cord and vertebral column. In: Chou SN, Seljeskog EL, eds. Seminars in neurological surgery. Spinal deformities and neurological dysfunction. New York: Raven, 1978; 1–10.
12. Lott G, Klein E. Osteopetrosis: A case presentation. AJR 1965; 94:616–620.
13. Maroteaux P, Lamy M. Hurler's disease, Morquio's disease, and related mucopolysaccharidosis. J Pediatr 1965; 67:312–323.
14. Martel W, Holt JF, Cassidy JT. Roentgenologic manifestations of juvenile rheumatoid arthritis. AJR 1962: 88:400–423.
15. Mitchell GE, Lourie H, Berne AS. The various causes of scalloped vertebrae with notes on their pathogenesis. Radiology 1967; 89:67–74.
16. Murray RO. Steroids and the skeleton. Radiology 1961; 77:729–743.
17. Neuhauser EBD, Wittenborg MH, Berman CZ, Cohen J. Irradiation effects of roentgen therapy on growing spine. Radiology 1952; 59:637–650.
18. Resnick D, Niwayama G. Diagnosis of bone and joint disorders. Philadelphia: Saunders, 1981.
19. Reynolds J, Pritchard JA, Ludders D, Mason RA. Roentgenographic and clinical appraisal of sickle-cell and beta-thalassemia disease. AJR 1973; 118:378–400.
20. Rourke JA, Heslin DJ. Gaucher's disease. AJR 1965; 94:621–630.
21. Schmorl G, Junghanns H. The human spine in health and disease. 2d ed. New York: Grune & Stratton, 1971.
22. Yaghmai I. Spinal changes in neurofibromatosis. RadioGraphics 1986; 6:261–285.